Electronic Structure

OPEN ACCESS

PAPER

A unified secondary electron cut-off presentation and common mistakes in photoelectron spectroscopy

Thorsten Schultz*

Humboldt-Universität zu Berlin, Institut für Physik, 12489 Berlin, Germany
Helmholtz-Zentrum Berlin für Materialien und Energie GmbH, 12489 Berlin, Germany
* Author to whom any correspondence should be addressed.

E-mail: thorsten.schultz@helmholtz-berlin.de

Keywords: work function, binding energy referencing, peak fitting

RECEIVED
30 August 2022

REVISED
18 October 2022

ACCEPTED FOR PUBLICATION
3 November 2022

PUBLISHED
17 November 2022

Abstract

Photoelectron spectroscopy is a powerful surface analysis technique that can differentiate different bonding environments and directly determine the absolute work function of a sample. Despite its ever-easier accessibility—or perhaps precisely because of it—some common mistakes or bad habits are often found in the literature when it comes to the evaluation or presentation of photoelectron spectroscopy data. Here we address some of these issues and give suggestions for best practice, i.e., a proper presentation of the secondary electron cut-off used for work function determination, correct binding energy referencing and some tips for appropriate peak fitting, as well as valuable literature references to more detailed tutorials. Finally, we present a concise step-by-step guide on how to conduct a complete x-ray photoelectron spectroscopy analysis of an unknown sample.

1. Introduction

Photoelectron spectroscopy was developed in 1957 by Siegbahn [1] and is based on the photoelectric effect. When a material is illuminated by highly energetic light $h\nu$, typically x-rays or UV-light, electrons are emitted [2]. Their kinetic energy E_k is measured by a detector and is given by: $E_k = h\nu - E_b - \Phi_D$, where E_b is the binding energy of the respective orbital and Φ_D is the work function of the detector. Plotting the number of detected electrons as a function of energy one can obtain a multitude of information like, e.g., elemental composition, the type of chemical bonds or the sample work function.

Judging from the numbers of publications per year (7590 in 1998, 16 500 in 2008 and 72 700 in 2018 [3]), photoelectron spectroscopy has become a frequently used technique over the past 20 years. The recent development of user-friendly, commercial, but at the same time black-box-like setups by many companies has given non-experts the means to easily conduct photoelectron spectroscopy measurements. This leads to a large variety in quality of the reported data and analysis. Here we want to make aware of some common mistakes and bad habits often observed in photoelectron spectroscopy literature, to sensitize both authors and reviewers to be more critical with data and its analysis/description. This covers the issues of a unified secondary electron cut-off (SECO) presentation for work function determination, a correct binding energy calibration/referencing, some tips for peak fitting and a concise step-by-step guide on how to conduct a complete x-ray photoelectron spectroscopy analysis of an unknown sample.

2. SECO presentation

Photoelectron spectroscopy is one of the few techniques that allows for a direct measurement of the absolute work function of a sample. This is achieved by measuring the intensity of the electrons with the lowest kinetic energy, the so-called secondary electron cut-off (SECO). These electrons have lost almost all their kinetic energy due to scattering events inside the sample and have just enough energy to overcome the work function of the sample and leave it.

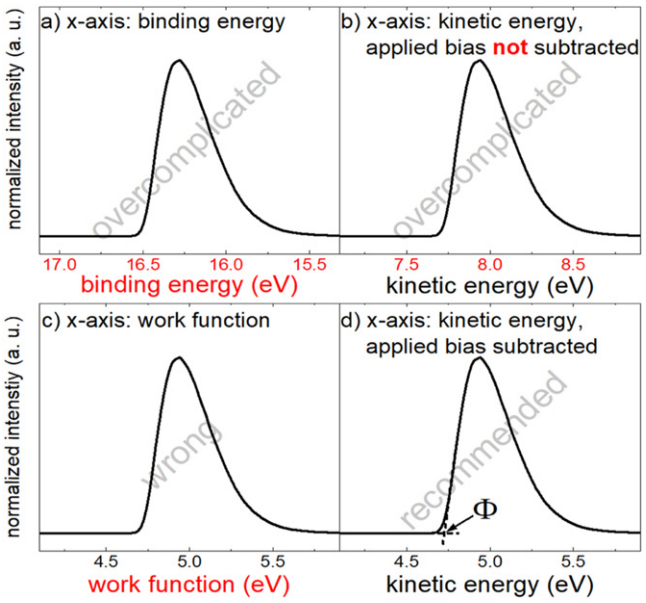

Figure 1. Different exemplary presentations of SECOs found in literature. The red highlighted parts exemplify errors/overcomplications. (a) The *x*-axis is plotted as binding energy. (b) The *x*-axis is plotted as kinetic energy, but the applied bias is not subtracted. (c) The *x*-axis is plotted as work function. (d) The *x*-axis is plotted as kinetic energy, with the applied bias already subtracted.

This manifests in a sharp onset and increase in intensity when scanning the low kinetic energy range. Helander *et al* [4] have demonstrated important experimental details to consider to conduct SECO measurements correctly and Schultz *et al* [5] have shown how to interpret SECO measurements of heterogeneous surfaces. Here we focus on proper presentation of SECO data for publication. There are four ways to present SECO data found in literature, exemplified in figure 1. The differences are the following:

(a) *x*-axis given as binding energy [6–13].

This presentation is one of the most frequently used in literature. The motive behind it most probably comes from the idea that the full ultraviolet photoelectron spectrum is plotted, from the Fermi-edge of the sample all the way to the SECO, as demonstrated in some photoelectron spectroscopy reviews or online tutorials [14–16], and one wants the Fermi-edge to be positioned at 0 eV binding energy. However, in most publications only the SECO is plotted separately. This presentation has the disadvantage that a direct reading of the work function value is overcomplicated, as one first has to look up the used excitation energy, which is sometimes not even stated [9].

(b) *x*-axis given as kinetic energy, but the applied bias is not subtracted [17, 18].

During a SECO measurement a negative bias should be applied to the sample for two reasons: (1) If the work function of the sample is smaller than the work function of the detector (typically around 4 eV) the slowest electrons are not able to reach the detector. They need additional energy in the form of an applied bias. This is usually reported with the following phrase: *to overcome the detector work function*. (2) Photoelectrons traveling through the analyzer can themselves again excite electrons from, e.g., the analyzer walls, which results in an additional SECO signal corresponding to the analyzer work function. The applied bias only shifts the electrons stemming from the sample, not the ones created inside the analyzer, therefore separating the true SECO signal from the artificial one. This is usually referred to as *clearing the analyzer work function*. If the bias is not subtracted before plotting, the reader has to look up the applied bias, usually given in the experimental section or not at all [9, 11, 19], again overcomplicating the direct reading of the work function value.

(c) *x*-axis given as work function [19, 20].

This is the only presentation which is actually plain wrong. The work function of the sample is only one single point in the diagram, given by the intersection of the flat background and a linear extrapolation of the steep slope as shown in figure 1(d). The detector measures the number of electrons (intensity) as a function of their kinetic (or binding) energy, which only allows the *x*-axis to be one of these two.

(d) *x*-axis given as kinetic energy, with the applied bias already subtracted

We suggest experimentalists and reviewers to use and only accept this form of presentation for SECO spectra. It allows a direct extraction of the work function value by the reader without the need to look up additional information. This information though, i.e., excitation energy and applied bias, should still be given in the experimental section.

3. Binding energy referencing

A correct binding energy reference is essential for a comparison of measurements between different setups. Unfortunately, there are still some publications which do not state the used referencing method at all [21, 22]. These data are not useable for comparison and should be rejected by reviewers. There are typically three methods of binding energy referencing:

(a) Fermi-edge

Metallic samples show a distinct Fermi-edge, which is set to 0 eV binding energy as a reference. This is typically used for ultraviolet photoelectron spectrsocpy (UPS) measurements. For XPS measurements, the cross section of these electrons, and therefore the signal intensity, is usually very small. Therefore, the next method is more often used for XPS measurements.

(b) Core level binding energies

Some core levels of metals have been established as reliable source for binding energy referencing. These are typically the $Au4f_{7/2}$ core level set to 83.95 eV, the $Ag3d_{5/2}$ core level set to 368.22 eV or the $Cu2p_{3/2}$ core level set to 932.62 eV [23]. A proper linearity of the binding energy scale is ensured by calibrations using two core levels with a large energy difference, like the $Au4f_{7/2}$ and the $Cu2p_{3/2}$ core levels. A lot of setups have already an automated self-calibration function built in [24]. For this method to be reliable the reference samples need to be purely metallic, properly cleaned, e.g., by argon sputtering, and electrically well connected to the analyzer.

(c) Adventitious carbon (AdC)

A lot of studies on semiconducting or insulating samples use this method as a binding energy reference, because the samples are charging (built up of positive charge at the sample surface due to a lack of compensation of emitted photoelectrons, accompanied by a shift of all peaks to higher binding energies) and the two methods described above only work for samples which are sufficiently conductive. Here, the binding energy of the C1s core level of an AdC layer, which is typically present on all samples which have been exposed to air or have been stored in vacuum for some time [25, 26], is set to a specific value and all other peaks are shifted accordingly. Typical values found in literature are 284.5 eV, 284.8 eV or 285.0 eV. Greczynski *et al* presented a nice overview of the drawbacks of the AdC method [26, 27]. They demonstrated that the binding energy of the AdC C1s core level depends on the work function of the substrate and that it can vary between 284.08 eV and 286.74 eV. They criticize this method in such a way that they even say: '*No method is, however, better than an incorrect method*'. [26]. However, Biesinger demonstrated recently that the C1s method lead to satisfactory results in 95% of the cases [28]. It is therefore necessary to raise the awareness of when it is, up to date, unavoidable to use this method and how to interpret the obtained data. For example: a direct assignment of the chemical state by comparison to literature must be avoided, however, the differentiation of multiple chemical states present in the sample could still be successfully done. And elemental composition determination as well as chemical identification with the help of the Auger parameter [29] are always possible, no matter the referencing method. Anyhow, a proper description of the measurement setup, the energy referencing as well as the sample history, as suggested in form of a template by Greczynski and Hultman [26], should become standard for publications including photoelectron spectroscopy data.

4. Peak fitting

The differentiation and quantification of chemical states often requires the deconvolution of a measured signal, a procedure called *peak fitting*. This procedure requires some experience, but there are good overviews of proper peak fitting strategies, e.g., by Singh *et al* [30], Shard [31] or Major and colleagues [32]. Here we would like to briefly address some mistakes which can be easily avoided:

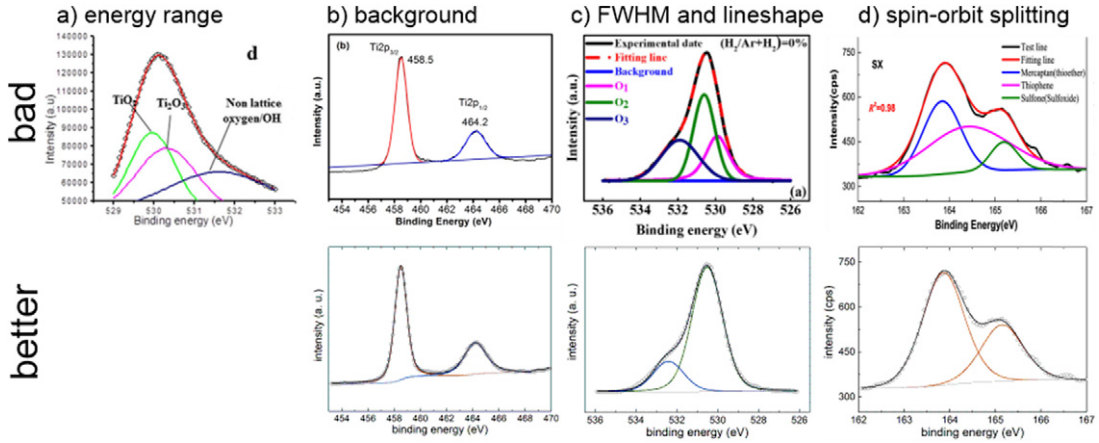

Figure 2. Things to consider when peak fitting XPS spectra. The top row shows bad examples from literature, the bottom row shows better fits to the same data. (a) The measured energy range is too small. Reproduced from [21]. CC BY 4.0. (b) The start and end points for the background are not selected properly, therefore the background lies above the data at some points. Reproduced from [36]. CC BY 4.0 .(c) The full width at half maximum (FWHM) and line shapes of the components are significantly different, leading the authors to the conclusion that there are three peaks needed to fit the spectra, while only two peaks would be sufficient. Adapted from [39], with permission from Springer Nature. (d) The spin–orbit splitting of the S2p core level into $S2p_{1/2}$ and $S2p_{3/2}$ has not been considered, leading to the wrong assignment of multiple chemical species. [44] John Wiley & Sons. © 2020 Curtin University and John Wiley & Sons, Ltd.

(a) Too narrow an energy range

If the measured energy range is chosen too narrow, as for example shown in figure 2(a) [21], a meaningful analysis of the data is often not possible, as a proper background cannot be applied. An appropriate measurement range is typically at least about ±2 eV above/below the onsets of the investigated peaks.

(b) Incorrect background subtraction

In the newest version of CasaXPS [33], a commercial XPS analysis software, are more than 80! types of backgrounds available to choose from. Therefore, it is not surprising that the choice of a proper background can be difficult for XPS novices. The most common types of background used in the XPS community are linear, Shirley or Tougaard backgrounds. All of them have their advantages and drawbacks and none is physically one hundred percent correct. A good review on XPS backgrounds in general is given by Engelhard and colleagues [34] and a recent review with more focus on the Tougaard background by Tougaard himself [35]. No matter the chosen background type, some criteria should always be met:

1. The background should never exceed the data, as shown in figure 2(b) [36].
2. The type of background used should be the same for comparable samples.
3. The area ratio of spin–orbit pairs should come out as theoretically expected (see paragraph 4 for more details).

(c) Incorrect full widths at half maximum (FWHMs) and peak shapes

The shape and FWHM of a peak depend on different factors and are typically a convolution of the natural line width, caused by the core-hole lifetime broadening (Lorentzian shape), and the setup broadening (x-ray source and analyzer, typically Gaußian shape), therefore a Voigt-function is often assumed for XPS peaks [37]. In the case of asymmetric peak shapes, e.g., present for pure metals, Doniach–Šunjić or asymmetric pseudo-Voigt functions are used [38]. Some things to consider about FWHMs and line-shapes:

1. The FWHM and shape of the same peak should not change significantly when comparing similar samples.
2. For the same oxidation states within one sample the FWHMs and peak shapes should be similar, in contrast to what was used to fit the O1s peak of ZnO in figure 2(c). [39]. Considering this allows to fit the spectrum with only two peaks, typically observed for ZnO and representing the bulk oxygen and the surface −OH groups [40].
3. Oxide species typically have a wider, symmetric line-shape, while pure metallic peaks are narrower and often asymmetric.

4. Typical peak FWHM values are 0.6–3 eV. Anything much smaller or larger than that should be critically examined.
5. A collection of natural line widths for atomic K-N7 levels is given by Campbell and Papp [41].

(d) Neglecting spin–orbit splitting

A coupling between angular momentum **L** and spin angular momentum **S** leads to a splitting of the energy levels into two states for all transitions with $l > 0$. The degeneracy of these energy levels leads to a fixed area ratio between the observed doublets, as given in the following table:

Subshell	j values ($j = l \pm s$)	Area ratio
p ($l = 1$)	1/2 & 3/2	1:2
d ($l = 2$)	3/2 & 5/2	2:3
f ($l = 3$)	5/2 & 7/2	3:4

The energy difference between the two peaks is constant for each doublet, but can vary for different oxidation states [42]. Literature values can be found in the NIST XPS database [43]. Including the spin–orbit splitting with the corresponding constraints during fitting is essential, especially when the energy difference is smaller than the chemical shift for different oxidation states. An example of how the neglection of a spin–orbit doublet can lead to an erroneous assignment of chemical species is shown in the S2p spectrum in figure 2(d) [44].

XPS users should internalize that **a meaningful physical model is much more important than a convulsive perfect fit to the data**. As a good starting point for any XPS measurement and attempt to peak fitting we personally recommend the XPS reference page from the University of Western Ontario [45] and the periodic table from ThermoFisher [46].

5. A step-by-step guide for XPS measurements and analysis

We would like to give the readership a concise step-by-step guide on how to conduct XPS measurements and data evaluation on an unknown sample, similar to pages 40–42 in [47]. A very detailed step-by-step tutorial on how to prepare, conduct and evaluate XPS experiments was just recently published by Greczynski and Hultman [47] and is recommended for more information. Here we focus on sufficiently conductive thin film samples, assume that a proper calibration of the system has been carried out already (for details on how to do that see section 3) and neglect *in situ* sample preparation.

Measurement:

(a) Sample mounting: The sample should be mounted in a way that the surface is in electrical contact with the sample holder. This helps to avoid charging and can, e.g., be realized by screws, clamps or conductive tape.

(b) Survey scan: To get an overview of the elements present in the sample, typically a wide range scan is performed first. A binding energy range between 1100 to 0 eV covers all potential elements. As the signal intensity is of primary concern here, a high pass energy and an energy step size of 0.5–1 eV are typically chosen for such a scan.

(c) Peak identification: Most measurement and evaluation programs, like CasaXPS [33], have a built-in element library, which helps to identify the peaks in the survey spectrum. If not, the NIST XPS database [43] can be used to identify unknown peaks. One should be aware of shake-up lines, energy loss lines and x-ray satellites and ghost lines for achromatic x-ray sources, which can complicate the peak identification [48].

(d) Choice of excitation source: While core levels have a binding energy, which is independent of the excitation source, the binding energy position of Auger peaks varies with excitation energy. Therefore, they can overlap with the core level peaks of interest. If this is the case, switching to a different excitation source (if available) can help to overcome this problem.

(e) Narrow scans: After all elements have been identified from the survey spectrum the most intense core level peaks are scanned with better resolution for chemical state identification. Therefore, a smaller pass energy and energy steps of 50–200 meV are typically used. As described in section 4, the energy range should cover at least ±2 eV above/below the onsets of the investigated peaks for proper background application later. Measuring the Auger peaks as well can help to differentiate different chemical states with the help of the Auger parameter [29]. The number of scans should be adjusted in a way that a sufficient signal to noise ratio is achieved.

Analysis:

(f) **Peak fitting:** A deconvolution of the narrow scans to obtain information about different chemical bonds can be conducted, following the hints given in section 4 and the references therein.
(g) **Comparison to literature binding energies:** The identification of the different chemical states derived through peak fitting can be achieved by comparing the obtained binding energies with literature values of reference samples. This requires a proper binding energy scale calibration and should be avoided when using the AdC method.
(h) **Quantification:** The area of the measured peaks in combination with their sensitivity factors, which are usually provided by the manufacturer of the system, can yield a quantitative composition of the sample surface area. However, it should be kept in mind that this procedure assumes a homogeneous distribution of all elements and that overlayers, e.g. AdC, can influence the result due to different inelastic mean free paths of the different core levels.

Presentation:

(i) **Binding energy scale:** XPS spectra should be plotted with the binding energy decreasing from left to right.
(j) **Data and fits:** Raw data should be presented as symbols without a background being subtracted from them. The fitted peaks and their sum should be overlaid as solid lines for a direct assessment of the quality of the fit.

6. Conclusion

We suggest the preferred way to present SECO measurements for work function determination by photoemission spectroscopy, to hopefully achieve a common standard in the future. The correct plot shows the measured intensity of photoelectrons as a function of the kinetic energy of the emitted electrons, with an applied bias already subtracted. Furthermore, common mistakes in binding energy referencing and peak fitting are pointed out, which can be easily avoided, and references to more detailed tutorials are given. Finally, a concise step-by-step guide on how to conduct XPS measurements and data evaluation is provided. This work should sensitize authors as well as reviewers to critically pay attention to the quality of photoemission data and their evaluation and give beginners in the field a good starting point to avoid common mistakes.

Acknowledgments

The author thanks Steffen Duhm for fruitful discussions and Andreas Opitz and Ross Warren for revising the manuscript.

Data availability statement

The data that support the findings of this study are available upon reasonable request from the authors

ORCID iDs

Thorsten Schultz https://orcid.org/0000-0002-0344-6302

References

[1] Nordling C, Sokolowski E and Siegbahn K 1957 Precision method for obtaining absolute values of atomic binding energies *Phys. Rev.* **105** 1676–7
[2] Einstein A 1905 Über einen die Erzeugung und Verwandlung des Lichtes betreffenden heuristischen Gesichtspunkt *Ann. Phys.* **322** 132–48
[3] Google scholar search: number of publications including 'photoelectron spectroscopy' in the title.
[4] Helander M G, Greiner M T, Wang Z B and Lu Z H 2010 Pitfalls in measuring work function using photoelectron spectroscopy *Appl. Surf. Sci.* **256** 2602–5
[5] Schultz T *et al* 2017 Reliable work function determination of multicomponent surfaces and interfaces: the role of electrostatic potentials in ultraviolet photoelectron spectroscopy *Adv. Mater. Interfaces* **4** 1700324
[6] Hu J *et al* 2022 Tracking the evolution of materials and interfaces in perovskite solar cells under an electric field *Commun. Mater.* **3** 39

[7] Zhang H *et al* 2017 Origin of charge transfer and enhanced electron–phonon coupling in single unit-cell FeSe films on $SrTiO_3$ *Nat. Commun.* **8** 214
[8] Arnaud G F, De Renzi V, del Pennino U, Biagi R, Corradini V, Calzolari A, Ruini A and Catellani A 2014 Nitrocatechol/ZnO interface: the role of dipole in a dye/metal-oxide model system *J. Phys. Chem.* C **118** 3910–7
[9] Mahato S, Puigdollers J, Voz C, Mukhopadhyay M, Mukherjee M and Hazra S 2020 Near 5% DMSO is the best: a structural investigation of PEDOT: PSS thin films with strong emphasis on surface and interface for hybrid solar cell *Appl. Surf. Sci.* **499** 143967
[10] Jäckle S, Mattiza M, Liebhaber M, Brönstrup G, Rommel M, Lips K and Christiansen S 2015 Junction formation and current transport mechanisms in hybrid n-Si/PEDOT:PSS solar cells *Sci. Rep.* **5** 13008
[11] Lu L *et al* 2020 Interaction of the cation and vacancy in hybrid perovskites induced by light illumination *ACS Appl. Mater. Interfaces* **12** 42369–77
[12] Choi J Y, Heo K, Cho K S, Hwang S W, Chung J, Kim S, Lee B H and Lee S Y 2017 Effect of Si on the energy band gap modulation and performance of silicon indium zinc oxide thin-film transistors *Sci. Rep.* **7** 15392
[13] Hosokai T *et al* 2015 Thickness and substrate dependent thin film growth of picene and impact on the electronic structure *J. Phys. Chem.* C **119** 29027–37
[14] Olthof S 2021 The impact of UV photoelectron spectroscopy on the field of organic optoelectronics—a retrospective *Adv. Opt. Mater.* **9** 2100227
[15] Steirer X 2015 *A lesson in utraviolet photoelectron spectroscopy* https://energyscienceeducation.com/a-lesson-in-ultraviolet-photoelectron-spectroscopy/
[16] HarwellXPS 2018 *UPS: a highly surface sensitive technique for the analysis of valence bands and the workfunction of materials* https://subsite.harwellxps.uk/?page_id=256
[17] MacQueen R W *et al* 2018 Crystalline silicon solar cells with tetracene interlayers: the path to silicon-singlet fission heterojunction devices *Mater. Horiz.* **5** 1065–75
[18] Niederhausen J, Amsalem P, Frisch J, Wilke A, Vollmer A, Rieger R, Müllen K, Rabe J P and Koch N 2011 Tuning hole-injection barriers at organic/metal interfaces exploiting the orientation of a molecular acceptor interlayer *Phys. Rev.* B **84** 165302
[19] Shamieh B, Anselmo A S, Vogel U, Lariou E, Hayes S C, Koch N and Frey G L 2018 Correlating the effective work function at buried organic/metal interfaces with organic solar cell characteristics *J. Mater. Chem.* C **6** 8060–8
[20] Tirado J, Vásquez-Montoya M, Roldán-Carmona C, Ralaiarisoa M, Koch N, Nazeeruddin M K and Jaramillo F 2019 Air-stable n–i–p planar perovskite solar cells using nickel oxide nanocrystals as sole hole-transporting material *ACS Appl. Energy Mater.* **2** 4890–9
[21] Bharti B, Kumar S, Lee H N and Kumar R 2016 Formation of oxygen vacancies and Ti^{3+} state in TiO_2 thin film and enhanced optical properties by air plasma treatment *Sci. Rep.* **6** 32355
[22] Didwal P N, Chikate P R, Bankar P K, More M A and Devan R S 2019 Intense field electron emission source designed from large area array of dense rutile TiO_2 nanopillars *J. Mater. Sci., Mater. Electron.* **30** 2935–41
[23] Seah M P 2001 Summary of ISO/TC 201 Standard: VII ISO 15472: 2001—surface chemical analysis—x-ray photoelectron spectrometers—calibration of energy scales *Surf. Interface Anal.* **31** 721–3
[24] Thermo Scientific 2008 Thermo scientific, K-alpha: energy scale linearity and calibration http://tools.thermofisher.com/content/sfs/brochures/D16127.pdf (accessed 18 October 2022)
[25] Greczynski G and Hultman L 2022 Impact of sample storage type on adventitious carbon and native oxide growth: x-ray photoelectron spectroscopy study *Vacuum* **205** 111463
[26] Greczynski G and Hultman L 2020 X-ray photoelectron spectroscopy: towards reliable binding energy referencing *Prog. Mater. Sci.* **107** 100591
[27] Greczynski G and Hultman L 2022 Undressing the myth of apparent constant binding energy of the C1s peak from adventitious carbon in x-ray photoelectron spectroscopy *Sci. Talks* **1** 100007
[28] Biesinger M C 2022 Accessing the robustness of adventitious carbon for charge referencing (correction) purposes in XPS analysis: insights from a multi-user facility data review *Appl. Surf. Sci.* **597** 153681
[29] Shima M, Tsutsumi K, Tanaka A, Onodera H and Tanemura M 2018 Chemical state analysis using Auger parameters for XPS spectrum curve fitted with standard Auger spectra *Surf. Interface Anal.* **50** 1187–90
[30] Singh B, Hesse R and Linford M R 2015 Good practices for XPS (and other types of) peak fitting *Vac. Technol. Coat.* **16** 25–31
[31] Shard A G 2020 Practical guides for x-ray photoelectron spectroscopy: quantitative XPS *J. Vac. Sci. Technol.* A **38** 041201
[32] Major G H, Fairley N, Sherwood P M A, Linford M R, Terry J, Fernandez V and Artyushkova K 2020 Practical guide for curve fitting in x-ray photoelectron spectroscopy *J. Vac. Sci. Technol.* A **38** 061203
[33] Fairley N *et al* 2021 Systematic and collaborative approach to problem solving using x-ray photoelectron spectroscopy *Appl. Surf. Sci. Adv.* **5** 100112
[34] Engelhard M H, Baer D R, Herrera-Gomez A and Sherwood P M A 2020 Introductory guide to backgrounds in XPS spectra and their impact on determining peak intensities *J. Vac. Sci. Technol.* A **38** 063203
[35] Tougaard S 2021 Practical guide to the use of backgrounds in quantitative XPS *J. Vac. Sci. Technol.* A **39** 011201
[36] Xie W, Li R and Xu Q 2018 Enhanced photocatalytic activity of Se-doped TiO_2 under visible light irradiation *Sci. Rep.* **8** 8752
[37] Jain V, Biesinger M C and Linford M R 2018 The Gaussian–Lorentzian sum, product, and convolution (Voigt) functions in the context of peak fitting x-ray photoelectron spectroscopy (XPS) narrow scans *Appl. Surf. Sci.* **447** 548–53
[38] Schmid M, Steinrück H P and Gottfried J M 2014 A new asymmetric pseudo-Voigt function for more efficient fitting of XPS lines *Surf. Interface Anal.* **46** 505–11
[39] Jiang Z *et al* 2022 Fabrication of high-performance ZnO-based thin-film transistors by Mg/H co-doping at room temperature *J. Mater. Sci., Mater. Electron.* **33** 2080–9
[40] Schlesinger R *et al* 2013 Controlling the work function of ZnO and the energy-level alignment at the interface to organic semiconductors with a molecular electron acceptor *Phys. Rev.* B **87** 155311
[41] Campbell J L and Papp T 2001 Widths of the atomic K-N7 levels *At. Data Nucl. Data Tables* **77** 1–56
[42] Biesinger M C, Lau L W M, Gerson A R and Smart R S C 2010 Resolving surface chemical states in XPS analysis of first row transition metals, oxides and hydroxides: Sc, Ti, V, Cu and Zn *Appl. Surf. Sci.* **257** 887–98
[43] Naumkin A V, Kraut-Vass A, Gaarenstroom S W and Powell C J 2000 *NIST X-Ray Photoelectron Spectroscopy Database, NIST Standard Reference Database Number 20* (Gaithersburg MD: National Institute of Standards and Technology) p 20899
[44] Ge T, Li F and Li Y 2021 Influence of dielectric property of organic sulfur compounds on coal microwave desulfurization, Asia-Pacific *J. Chem. Eng.* **16** e2581
[45] Biesinger M C 2009 *X-ray photoelectron spectroscopy (XPS) reference pages* http://xpsfitting.com/http://xpsfitting.com/

[46] Thermo Fisher Scientific 2022 *Table of elements: x-ray photoelectron spectroscopy of atomic elements* https://thermofisher.com/de/de/home/materials-science/learning-center/periodic-table.html
[47] Greczynski G and Hultman L 2022 A step-by-step guide to perform x-ray photoelectron spectroscopy *J. Appl. Phys.* **132** 11101
[48] Moulder J F, Stickle W F, Sobol P E and Bomben K D 1995 *Handbook of X-Ray Photoelectron Spectroscopy* (Eden Prairie: Physical Electronics, Inc.) pp 17–20